J Neurophysiol 91: 2079–2089, 2004;
10.1152/jn.01197.2003.

Low-Probability Transmission of Neocortical and Entorhinal Impulses Through the Perirhinal Cortex

Joe Guillaume Pelletier, John Apergis, and Denis Paré
Center for Molecular and Behavioral Neuroscience, Rutgers University, Newark, New Jersey 07102

Submitted 11 December 2003; accepted in final form 6 January 2004

Pelletier, Joe Guillaume, John Apergis, and Denis Paré. Low-probability transmission of neocortical and entorhinal impulses through the perirhinal cortex. *J Neurophysiol* 91: 2079–2089, 2004; 10.1152/jn.01197.2003. One model of episodic memory posits that during slow-wave sleep (SWS), the synchronized discharges of hippocampal neurons in relation to sharp waves "replay" activity patterns that occurred during the waking state, facilitating synaptic plasticity in the neocortex. Although evidence of replay was found in the hippocampus in relation to sharp waves, it was never shown that this activity reached the neocortex. Instead, it was assumed that the rhinal cortices faithfully transmit information from the hippocampus to the neocortex and reciprocally. Here, we tested this idea using 3 different approaches. *1*) Stimulating electrodes were inserted in the entorhinal cortex and temporal neocortex and evoked unit responses were recorded in between them, in the intervening rhinal cortices. In these conditions, impulse transfer occurred with an extremely low probability, in both directions. *2*) To rule out the possibility that this unreliable transmission resulted from the artificial nature of electrical stimuli, crosscorrelation analyses of spontaneous neocortical, perirhinal, and entorhinal firing were performed in unanesthetized animals during the states of waking and SWS. Again, little evidence of propagation could be obtained in either state. *3*) To test the idea that propagation occurs only when large groups of neurons are activated within a narrow time window, we computed perievent histograms of neocortical, perirhinal, and entorhinal neuronal discharges around large-amplitude sharp waves. However, these synchronized entorhinal discharges also failed to propagate across the perirhinal cortex. These findings suggest that the rhinal cortices are more than a relay between the neocortex and hippocampus, but rather a gate whose properties remain to be identified.

INTRODUCTION

The perirhinal cortex is an elongated cortical strip located in the lateral bank (area 36) and fundus (area 35) of the rhinal sulcus. The perirhinal cortex occupies a strategic location in the temporal lobe because, together with the postrhinal cortices (Burwell and Witter 2002), it relays most neocortical sensory inputs to the entorhinal–hippocampal system. Moreover, it represents the main return path for hippocampo-entorhinal efferents to the neocortex (reviewed in Witter et al. 2000).

In particular, tract-tracing studies have revealed that information transfer between the neocortex and hippocampus depends on the sequential, stepwise activation of the perirhinal and entorhinal cortices (neocortex to area 36 to area 35 to entorhinal cortex to hippocampus and conversely). However, the progression of impulse traffic into discrete steps is not perfect, given that some deep neocortical neurons project beyond area 36 into area 35 and the lateral entorhinal cortex (Burwell and Amaral 1998a,b; Insausti et al. 1987; McIntyre et al. 1996; Saleem and Tanaka 1996; Suzuki and Amaral 1994; VanHoesen and Pandya 1975; reviewed in Burwell and Witter 2002). Similarly, some entorhinal axons extend to area 36 and the temporal neocortex (Burwell and Amaral 1998b; Deacon et al. 1983; Insausti et al. 1997; Suzuki and Amaral 1994; Swanson and Köhler 1986; reviewed in Burwell and Witter 2002).

Although little physiological work has been performed on this issue, it is typically assumed that the rhinal cortices (here defined to include the perirhinal, postrhinal, and entorhinal cortices) faithfully transmit neocortical inputs to the hippocampus and reciprocally. In fact, some models of episodic memory rest on this assumption. In the two-stage model of episodic memory, for instance, it is hypothesized that during waking, information of neocortical origin is initially stored in the hippocampus by changes in the strength of connections between pyramidal neurons. Later on during slow-wave sleep (SWS), the synchronized discharges of CA3 neurons in relation to sharp waves would "replay" representations stored in CA3 and, by activation of the rhinal cortices, reactivate neocortical neurons representing the event of interest (Buzsáki 1989). Ultimately, such SWS replay of waking activities would lead to long-term synaptic changes in the associative cortical networks that store memories (Buzsáki 1989; Pennartz et al. 2002).

Although evidence of replay was obtained in the hippocampus (Nadasdy et al. 1999; Skaggs and McNaughton 1996; Wilson and McNaughton 1994; reviewed in Sutherland and McNaughton 2000), whether hippocampal-driven activity is relayed by the perirhinal cortex back to neocortical storage sites has never been investigated before.

Thus determining the reliability of impulse transmission through the perirhinal cortex is an issue of crucial importance. Lesion and physiological studies already indicate that the perirhinal cortex plays a critical role in higher-order perceptual and/or mnemonic functions (Murray and Richmond 2001; Suzuki 1996), but its precise contribution, compared with that of the hippocampus, remains debated (Brown and Aggleton 2001).

The present study was undertaken to examine directly the transfer properties of the perirhinal cortex using multisite extracellular recordings as well as electrical stimulation of the temporal neocortex and entorhinal cortex. Our results suggest that the perirhinal cortex is not a passive relay station, but rather a gating or filtering network.

Address for reprint requests and other correspondence: D. Paré, CMBN, Aidekman Research Center, Rutgers, The State University of New Jersey, 197 University Ave., Newark, NJ 07102 (E-mail: pare@axon.rutgers.edu).

The costs of publication of this article were defrayed in part by the payment of page charges. The article must therefore be hereby marked "*advertisement*" in accordance with 18 U.S.C. Section 1734 solely to indicate this fact.

METHODS

Acute experiments

All procedures for acute experiments were approved by the Institutional Animal Care and Use Committee of Rutgers University, in compliance with the Guide for the Care and Use of Laboratory Animals (Department of Health and Human Services publication 86-23). Ten adult cats (2.5–3.5 kg) were preanesthetized with a mixture of ketamine and xylazine [15 and 2 mg/kg, intramuscularly (im)] and artificially ventilated with a mixture of ambient air, oxygen, and isoflurane. Atropine (0.05 mg/kg, im) was administered to prevent secretions. The end-tidal concentration in CO_2 was kept at 3.7 ± 0.2% and the body temperature was maintained at 37°C with a heating pad. The level of anesthesia was assessed by continuously monitoring the electroencephalogram and electrocardiogram. The bone overlying the rhinal region was removed and the dura mater opened.

To activate perirhinal and entorhinal neurons synaptically, an array of concentric stimulating electrodes was positioned in the band of neocortex that borders the perirhinal area laterally (Fig. 1*A*, *top row* of concentric circles). Similarly, concentric stimulating electrodes were positioned in the entorhinal cortex (Fig. 1*A*, *bottom row* of concentric circles). Evoked unit and field responses were recorded in between these 2 groups of stimulation sites by arrays of high-impedance microelectrodes (Fig. 1*A*, dots; 2-mm spacing; 2–6 MΩ at 1 kHz; OD = 80 μm; FHC, Brunswick, ME). These arrays were constructed by drilling small holes in a Teflon block and inserting the electrodes into them so that recordings could be obtained simultaneously from the perirhinal and entorhinal cortices. The block was attached to a micromanipulator and microelectrodes were lowered as a group in steps of 5 μm. See below for recording methods.

Experiments in unanesthetized animals

These experiments were carried out at Université Laval (Québec, Canada) in agreement with the guidelines of the Canadian Council for Animal Care. Adult cats were chronically implanted in a stereotaxic position under deep anesthesia in sterile conditions. The anesthesia was induced with ketamine (15 mg/kg, im), and atropine sulfate (0.05 mg/kg, im) was administered to prevent secretions. Then, sodium pentobarbital was injected gradually [Somnotol, ≈15 mg/kg, intravenously (iv)]. To record eye movements [electrooculogram (EOG)], two silver-ball electrodes were fixed into the supraorbital cavity with dental cement. Two Teflon-insulated wires were inserted in the neck muscles to monitor electromyographic activity (EMG), and stainless steel screws were anchored to the bone overlying the pericruciate area to monitor the electroencephalogram (EEG).

Then, arrays of tungsten electrodes were lowered until the electrodes reached the deep layers of the rhinal cortices (for details see Collins and Paré 1999). The array was constructed as above with the exception that the Teflon block was inserted in a tightly fitting Delrin sleeve, which was cemented to the bone. During the recording sessions, the electrodes could be lowered as a group by means of a micrometric screw. The lengths of electrodes were adjusted so that unit recordings could be obtained simultaneously from the temporal neocortex and both perirhinal and entorhinal cortices.

Finally, four screws were cemented to the skull. These screws were later used to fix the cat's head in a stereotaxic position without pain or pressure. Penicillin (20,000 IU/kg, im) and buprenorphine (0.03 mg/kg, im every 12 h for 24 h) were administered postoperatively. Recording sessions began 6 to 8 days after the surgery. In between experimental sessions, the animals slept, ate, and drank without restriction. During the recording sessions, behavioral states of vigilance were distinguished on the basis of previously described electrographic criteria (Steriade and Hobson 1976).

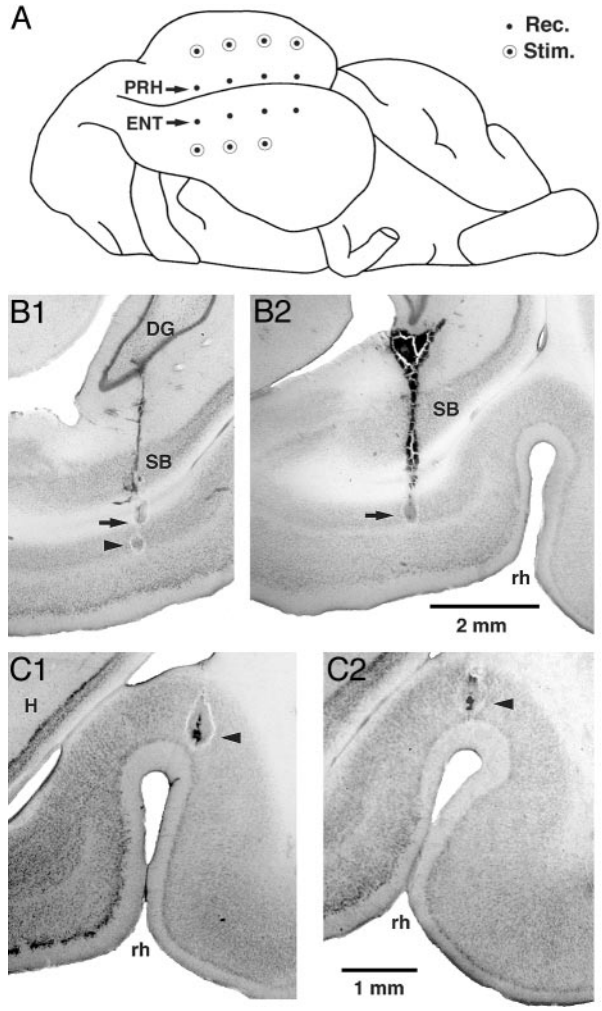

FIG. 1. Experimental setup and histological verification of recording sites. *A*: scheme of the ventral aspect of the cat brain showing the position of recording electrodes (Rec., dots) in the perirhinal (PRH) and entorhinal (ENT) cortices as well as the location of stimulating electrodes (Stim., concentric circles) in the temporal neocortex (*top row*) and entorhinal cortex (*bottom row*). *B–C*: histological verification of recording sites in the entorhinal (*B*) and perirhinal (*C*) cortices. At the end of experiments, the electrodes were pulled back to their starting position and this location was marked with an electrolytic lesion (arrows). In some tracks, lesions were made at a site where a particularly interesting neuron was recorded (arrowheads). Abbreviations: DG, dentate gyrus; H, hippocampus; rh, rhinal sulcus; SB, subiculum.

Recording methods

During the experiments, electrodes were lowered as a group. Neuronal activity was sampled at ≥100-μm intervals. Each time the electrodes were moved to a new recording site, 15–30 min elapsed before data were acquired, to ensure mechanical stability. The signals picked up by the electrodes (0.1 Hz to 20 kHz) as well as EEG, EMG, and EOG activity (in the case of chronic experiments) were observed on an oscilloscope, digitized, and stored on a hard disk. When evoked activity was studied, 30 to 300 shocks were delivered at each stimulation site, depending on the reliability of unit responses (the less reliable the response, the greater the number of shocks).

Histological identification of recording and stimulating sites

At the end of the experiments, recording sites were marked with electrolytic lesions (0.5 mA for 5 s). After this, the animals were given an overdose of sodium pentobarbital (50 mg/kg, iv) and perfused with

a cold saline solution (0.9%) followed by a solution containing 2% paraformaldehyde and 1% glutaraldehyde in 0.1 M phosphate buffer saline (pH 7.4). The brains were later sectioned on a vibrating microtome (at 100 μm) and stained with thionin or neutral red to verify the position of the recording electrodes. The microelectrode tracks were reconstructed by combining micrometer readings with the histology.

Analysis

Analyses were performed off-line with commercial software (IGOR, Wavemetrics, Lake Oswego, Oregon) and homemade software running on Macintosh computers. Spikes were detected using a window discriminator after digital filtering (0.3–20 kHz) of the raw waves. We considered only easily distinguishable neurons with a signal to noise ratio $\geq$3. Perievent histograms (PEHs) of unit discharges were computed. All values are expressed as means $\pm$ SE.

In the chronic experiments, crosscorrelograms of unit discharges were computed for all simultaneously recorded cell pairs (bins of 1 or 10 ms; range of $\pm$200 ms and $\pm$1 s, respectively) in waking and SWS. To be included in the analysis, neurons had to fire at $\geq$0.1 Hz in the particular behavioral state under consideration. Crosscorrelograms were then normalized to an average count of 1 and pooled in separate population histograms, depending on the position of the reference neurons and the distance between recorded cells.

RESULTS

Acute experiments

RESPONSIVENESS OF PERI- AND ENTORHINAL NEURONS TO NEOCORTICAL STIMULI. The effect of neocortical stimuli was tested in 584 perirhinal and 586 entorhinal neurons. Examples of histologically identified recording sites are provided in Fig. 1, *B* and *C*. Neocortical stimuli were much more efficient in orthodromically activating perirhinal (Fig. 2) than entorhinal (Fig. 3) neurons. Indeed, 39% of perirhinal cells (or 228 cells) could be synaptically activated from one or more neocortical stimulation sites (average latency of 12.9 $\pm$ 0.87 ms, Fig. 2*B*), compared with only 1.4% (or 8 cells) in the entorhinal cortex (average latency of 29.3 $\pm$ 4.4 ms). The difference in the proportion of responsive neurons was statistically significant ($\chi^2 = 254.8$, $P < 0.05$).

To test whether the likelihood of eliciting orthodromic responses varies with the laminar location of the cells (deep vs. superficial), neurons were separated according to their depth using histological controls. Entorhinal cells were grouped as either deep or superficial to the lamina dessicans, whereas perirhinal neurons in layers II–III were pooled separately from those in layers IV–VI. In the perirhinal cortex, the proportion of responsive cells was similar in deep (39%, $n = 309$) and superficial layers (40%, $n = 275$, $\chi^2 = 0.043$, $P > 0.05$). Similarly, no difference in the laminar distribution of cells responsive to neocortical stimuli was found in the entorhinal cortex (deep, 4 of 321; superficial, 4 of 265; $\chi^2 = 0.073$, $P > 0.05$).

The limited responsiveness of entorhinal neurons to neocortical stimuli was observed despite the fact that we routinely tested a large range of neocortical stimulation intensities (0.1–1.5 mA) and frequencies (0.01–300 Hz). Moreover, in an attempt to increase the likelihood of finding responsive entorhinal neurons, we stimulated a variety of neocortical sites (see Fig. 1*A*) one at a time or in pairs separated by various rostrocaudal distances (4, 8, or 12 mm in the rostrocaudal axis; see Fig. 1*A*), but without success.

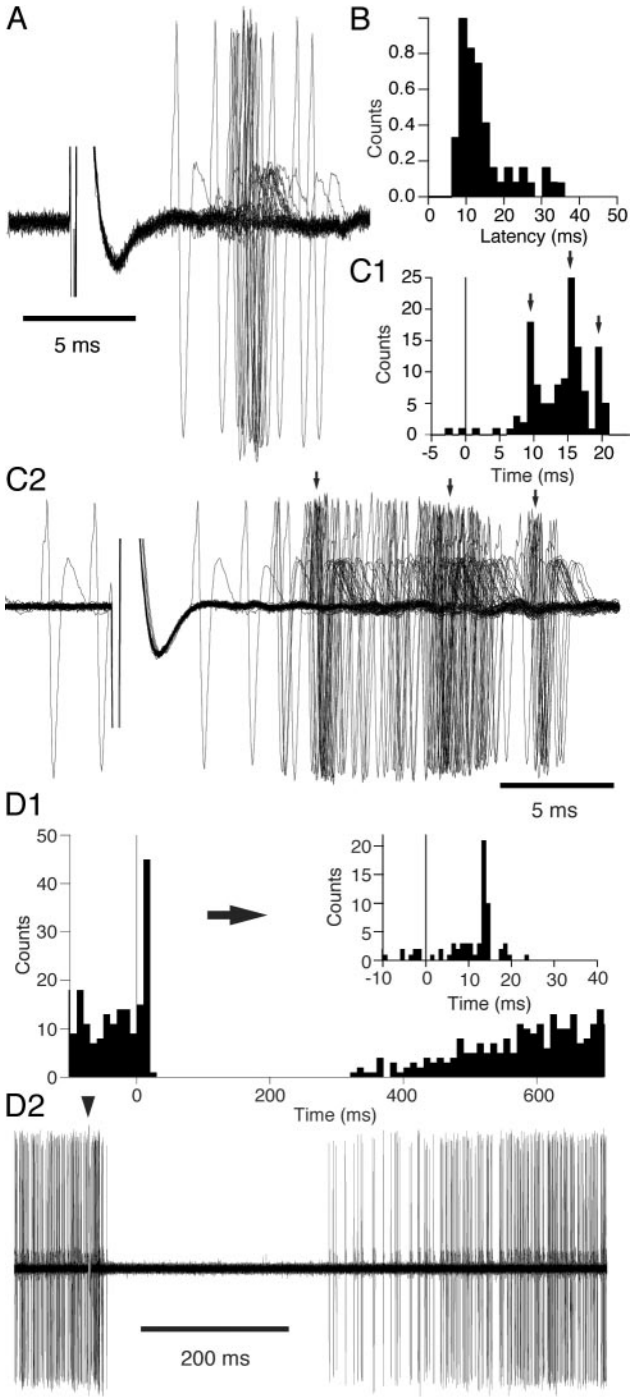

FIG. 2. Effect of neocortical stimuli on perirhinal neurons. *A*: short-latency orthodromic activation of a perirhinal neuron by a neocortical stimulus (31 superimposed trials). *B*: normalized frequency distribution of perirhinal response latencies after neocortical stimulation (228 cells). Histogram was normalized to the histogram mode. *C*: example of perirhinal cell in which neocortical shocks elicited orthodromic spikes that clustered at 3 different latencies (arrows). *C1*: *peristimulus histogram* (PSH) (61 stimuli). *C2*: superimposition of responses from which the histogram in *C1* was computed. *D*: neocortical stimuli also produced a prolonged suppression of firing in spontaneously firing neurons. *D1*: PSH (*left*: 10-ms bins; *right*: 1-ms bins) showing an example of such inhibition. *D2*: superimposition of responses from which the histograms in *D1* were computed (74 superimposed trials).

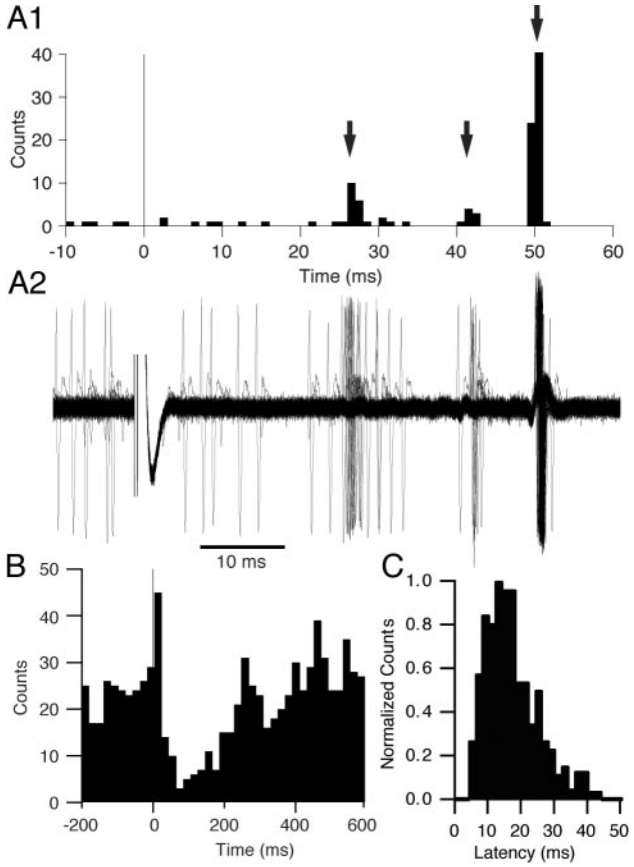

FIG. 3. Responses of entorhinal neurons to neocortical and entorhinal stimuli. *A*: example of entorhinal cell orthodromically responsive to neocortical stimuli. *A1*: PSH computed from 182 trials. *Rightmost mode* was truncated from 150 to 40 counts for clarity. *A2*: superimposition of responses from which the histogram in *A1* was computed. *B*: PSH showing that neocortical stimuli ($n = 375$) could also produce a prolonged suppression of firing in spontaneously firing entorhinal neurons. *C*: normalized frequency distribution of entorhinal latencies to entorhinal stimuli (38 cells). Histogram was normalized to the mode.

Examples of orthodromically activated perirhinal neurons are provided in Fig. 2, *A* and *C*. Most perirhinal neurons responded to neocortical stimuli with a relatively fixed latency (Fig. 2*A*). In fact, Fig. 2*C* illustrates the only example of perirhinal cell in which a multimodal peristimulus histogram (PSH) was observed. In contrast, half of responsive entorhinal neurons showed such multimodal poststimulus discharges (Fig. 3*A*; 4 out of 8 responsive cells). In these entorhinal cells, the interval between successive peaks averaged 10.8 ± 2.0 ms.

In spontaneously firing neurons (perirhinal, $n = 21$; entorhinal, $n = 32$), neocortical stimuli often produced long-lasting reductions in firing rate. In the perirhinal cortex, neocortical stimuli produced such inhibitions in all spontaneously active cells. The duration and amplitude of this inhibition increased with the stimulation intensity. Using stimuli of intermediate intensities (100 μs; 0.3 mA), the inhibition lasted 373 ± 21 ms and, at its peak, could transiently silence all cells (peak firing rate reduction of 100%). When neocortical stimuli evoked short-latency excitations (71% or 15 of 21 spontaneously firing cells), the inhibition developed immediately after the short-latency response (Fig. 2*D*). Neocortical stimuli also evoked an inhibition in the entorhinal cortex, albeit in a lower proportion of cells (59% or 19 of 32 spontaneously active cells). Otherwise, no differences in the duration (328 ± 18 ms) or magnitude (98 ± 1% decrease in instantaneous firing rate) of the inhibition was observed (*t*-test, $P > 0.05$).

RESPONSIVENESS OF ENTORHINAL AND PERIRHINAL NEURONS TO ENTORHINAL STIMULI. The results obtained with entorhinal stimuli were the mirror image of those seen with neocortical shocks. Indeed, no orthodromic activations were seen in as many as 271 tested perirhinal neurons compared with 19% of cells in the entorhinal cortex ($n = 201$; $\chi^2 = 55.72$, $P < 0.05$; average latency of 15.5 ± 1.1 ms; Fig. 3*C*). As was seen with neocortical stimuli, entorhinal shocks elicited a long-lasting inhibition of spontaneous firing. In subsets of spontaneously active entorhinal ($n = 41$) and perirhinal ($n = 22$) neurons, the proportion of cells showing a suppression of spontaneous activity after entorhinal stimuli was 68 and 14%, respectively.

Analysis of spontaneous discharges in unanesthetized animals

In the preceding experiments, it is possible that perirhinal and entorhinal responsiveness was affected by the anesthesia or the artificial nature of electrical stimuli. Thus we used a different approach to examine perirhinal transfer of neocortical and entorhinal impulses: we analyzed spontaneous neuronal activity in unanesthetized, head-restrained animals by means of an array of closely spaced microelectrodes in the temporal neocortex as well as the perirhinal and entorhinal cortices (Fig. 4*A*, *scheme*). This experiment was repeated 3 times and identical results were obtained.

Histological inspection of the electrode tracks confirmed that 195 of recorded cells were located in the entorhinal cortex, 126 in the perirhinal cortex, and 79 in the neocortex. Crosscorrelograms of unit discharges were computed for all simultaneously recorded cell pairs (bins of 1 or 10 ms). In doing so, the most laterally located cell was always considered as the reference neuron. Only cells recorded during waking and/or SWS and firing above 0.1 Hz were included in the analysis. Data obtained in paradoxical sleep was not considered because the animals spent too little time in this state.

FIG. 4. Crosscorrelation analysis of spontaneous activity in the states of waking (*A*) and slow-wave sleep (SWS) (*B–C*). Neurons were recorded using microelectrode arrays (*A, scheme).* To obtain the *population histograms* in *A* and *B,* crosscorrelograms of spontaneous discharges were computed for all simultaneously recorded cell pairs in all experiments. Individual crosscorrelograms were then normalized so that the mean bin value was equal to 1 and averaged depending on the position of the reference and target cells (numbers in the *upper left hand corner*). When correlating the activity of cells recorded by different electrodes, the reference cell was always the laterally located one. Asterisks indicate histograms with a significantly elevated bin within ±50 ms of the origin (paired *t*-test, $P < 0.05$). Numbers on the *top right* of the histograms indicate the number of cell pairs included in each analysis. Rhinal cells generally increased their firing rate during SWS, accounting for the discrepancy between the total number of crosscorrelograms in wake vs. SWS. *C*: graph plotting the proportion of crosscorrelograms with significant positive deviations (*y*-axis) from average bin values. A significance threshold of ±2.8 SDs was used. Proportion of significant histograms expected by chance is indicated by the thin dashed line. Abbreviations: DG, dentate gyrus; EC, entorhinal cortex; NC, neocortex; OT, optic tract; SBC, subiculum; V, ventricle.

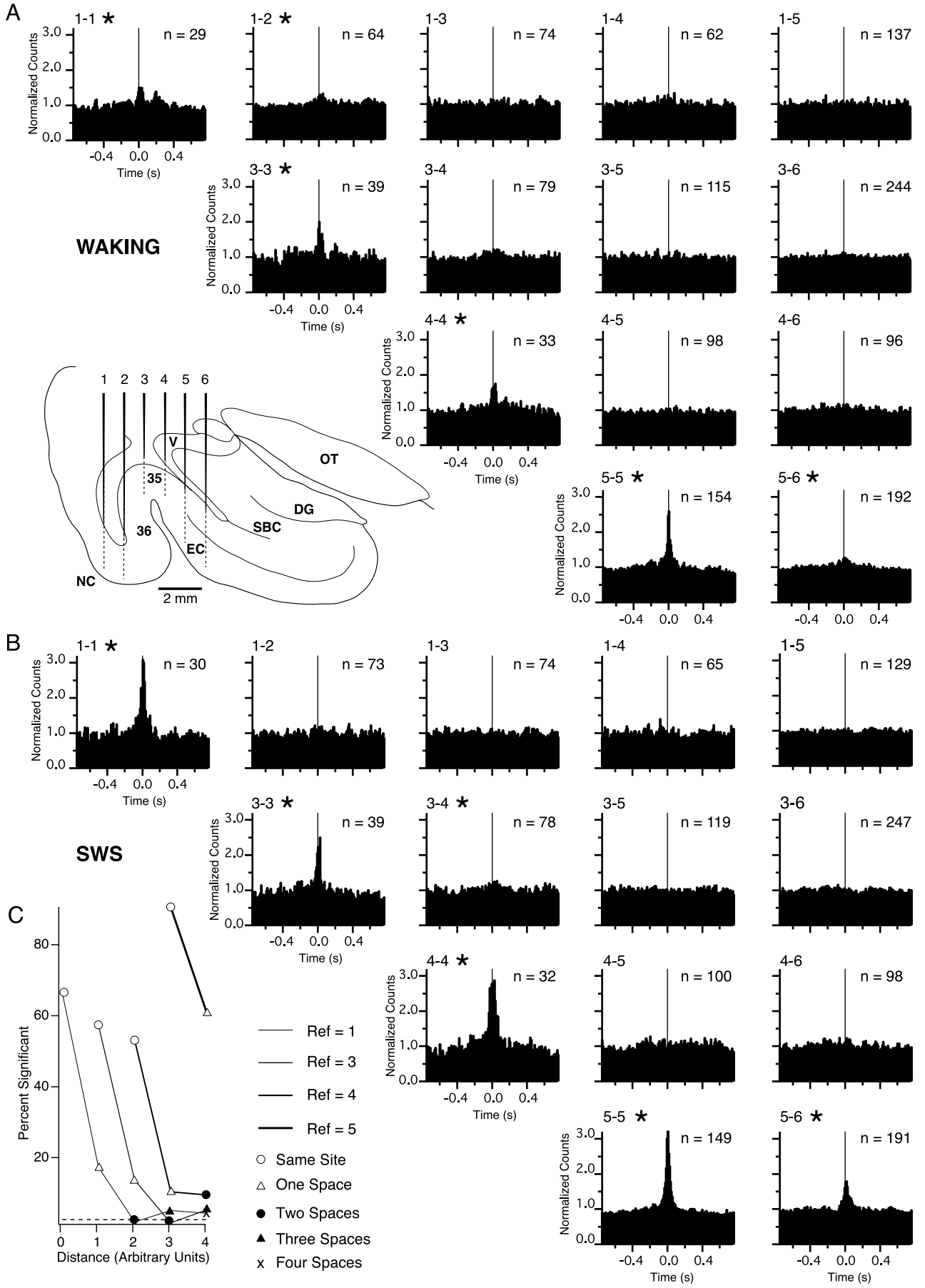
A
1-1 *
n = 29
1-2 *
n = 64
1-3
n = 74
1-4
n = 62
1-5
n = 137
3-3 *
n = 39
3-4
n = 79
3-5
n = 115
3-6
n = 244
WAKING
4-4 *
n = 33
4-5
n = 98
4-6
n = 96
5-5 *
n = 154
5-6 *
n = 192
Normalized Counts
Time (s)
1 2 3 4 5 6
V
OT
35
DG
SBC
36
EC
NC
2 mm
B
1-1 *
n = 30
1-2
n = 73
1-3
n = 74
1-4
n = 65
1-5
n = 129
3-3 *
n = 39
3-4 *
n = 78
3-5
n = 119
3-6
n = 247
SWS
4-4 *
n = 32
4-5
n = 100
4-6
n = 98
5-5 *
n = 149
5-6 *
n = 191
C
Percent Significant
Distance (Arbitrary Units)
Ref = 1
Ref = 3
Ref = 4
Ref = 5
Same Site
One Space
Two Spaces
Three Spaces
Four Spaces

SPATIAL EXTENT OF CORRELATED ACTIVITY IN WAKING AND SWS. If the stepwise connectivity that links the temporal neocortex and both peri- and entorhinal cortices allows propagation of signals to and from the hippocampus, one would expect crosscorrelograms of spontaneous firing to exhibit central peaks that decay as the distance between the recorded cells increases. Also, if the prevalent direction of propagation varies depending on the behavioral state, the peaks should gradually shift to the left or right as the distance between recorded cells increases. These ideas are tested below.

Figure 4 illustrates matrices of pooled crosscorrelograms for all simultaneously recorded cell pairs in the states of waking (Fig. 4*A*) and SWS (Fig. 4*B*). The numbers in the *upper left-hand corner* of the histograms indicate electrode positions used to record each cell pair (Fig. 4*A*, *scheme*). Asterisks indicate histograms with peaks (within ±50 ms of the origin) that reached statistical significance (paired *t*-test) at the 0.05 level after correction with the Bonferroni method for multiple comparisons.

In both waking (Fig. 4*A*) and SWS (Fig. 4*B*), evidence of synchronized firing was obtained in histograms correlating the activity of cells recorded from the same electrode. Such histograms had obvious peaks centered at around 0 ms (*t*-test, $P < 0.05$; Fig. 4, *A* and *B*). However, the peak amplitude of crosscorrelograms decreased sharply as the distance between the recorded cells increased. Indeed, at distances ≥1 mm, the differences between the histogram peaks and flanks generally did not reach significance. Identical results were obtained with bin widths of 1 and 10 ms.

Consistent with previous work in the neocortex (Steriade 1997) and hippocampus (Buzsáki et al. 1983), crosscorrelation of unit activity during SWS revealed a significant increase in synchrony relative to waking (*t*-test, $P < 0.05$). However, with the exception of entorhinal neurons (5–6 in Fig. 4, *A* and *B*), this increase in correlated activity was seen only for cells recorded at the same site.

In the preceding analysis, it is possible that some pairs of neurons had negatively or positively correlated activity but that averaging crosscorrelograms masked these relations. Also, variations in peak position might have led us to underestimate the amount of correlated activity. To examine these possibilities, individual crosscorrelograms were searched for bins (±50 ms from the origin) that deviated from the average bin value by ±2.8 SDs or more. This corresponds to the *z*-value required to reach significance in a 2-tailed *t*-test with $P < 0.05$ when performing 10 comparisons.

Figure 4*C* illustrates the result of this analysis for SWS data. This graph plots the proportion of crosscorrelograms with significant positive (*y*-axis) deviations from average bin values. Depending on the position of the reference cells, separate curves with different thickness are provided (see caption to the *right* of Fig. 4*C*). The various symbols indicate the distance between the recorded cells (see caption to the *right* of Fig. 4*C*). The dashed line indicates the proportion of significant correlograms expected by chance (2.5%). This analysis yielded results consistent with the population analysis.

The proportion of histograms with significant negative correlations remained below chance level and is not depicted in Fig. 4*C*. Thus the absence of positive correlations between distant cells in population crosscorrelograms did not result from cancellations between positive and negative correlations. With respect to positive correlations (Fig. 4*C*), the proportion of significant crosscorrelograms was highest for cells recorded by the same electrode (empty circles), irrespective of the position of the reference cell. With the exception of entorhinal neurons (thickest line, triangle), the proportion of significant histograms decreased below 20% with 1-mm separation (empty triangles). With longer distances, the proportion of significant correlograms varied with the position of reference neurons and target neurons. For neocortical and area 36 references, the proportion of significant correlograms decayed below chance level with 2-mm spacings and increased slightly to 4–5% with further interelectrode separations. However, with reference cells located in area 35, the proportion of significant correlograms remained as high as 11% with 2-mm spacings.

Thus the probability of correlated activity between neocortical and rhinal neurons is low but higher than expected by chance. Interhistogram variations in the position of the peak prevented detection of these correlations in population crosscorrelograms. Furthermore, for all spacings and reference sites, peaks of individual histograms occurred as frequently in the positive as in the negative direction. This result suggests that there is no prevalent direction of information flow between the neocortex and rhinal cortices.

It may be argued that the low incidence of correlated activity between distant neurons is a necessary consequence of signal attenuation along multisynaptic pathways (Shalden and Newsome 1998; Stevens and Zador 1998). However, the high proportion of significantly correlated activity among entorhinal neurons (Fig. 4*C*, thick line) led us to suspect that this might not be a general rule. Consistent with this, control experiments (Fig. 5*A*) revealed that a high proportion of entorhinal neurons separated by ≤3 mm display significantly correlated activity in waking and SWS. Figure 5*B* plots the proportion of entorhinal cell pairs with crosscorrelograms having bins (±50 ms from the origin) that deviated from the average bin value by ±2.8 SDs or more during SWS. Note that in contrast with neocortical and perirhinal cells (Fig. 4), a high proportion of significant crosscorrelograms was seen (≥25 times chance level). Moreover, evidence of this correlated activity was also present in population histograms (Fig. 5*C*).

RELATION BETWEEN LAMINAR LOCATION AND AMOUNT OF SYNCHRONY. It is possible that in the preceding analyses, the amount of synchrony was underestimated because we pooled deep and superficial cells. Indeed, deep and superficial rhinal layers receive distinct inputs (reviewed in Burwell and Witter 2002). To eliminate this possible confound, cells were separated according to their depth using histological controls. Entorhinal cells were grouped as either deep or superficial to the lamina dessicans, whereas perirhinal and neocortical neurons in layers II–III were pooled separately from those in layers IV–VI. In doing so, neurons located close to the border between deep and superficial layers were not considered to minimize the risk of errors. However, the depth of recorded neurons did not change the overall pattern of correlation in both waking and SWS. Whether the reference cells were located in the neocortex, perirhinal cortex, or entorhinal cortex, results were indistinguishable from those obtained in Fig. 4.

NETWORK ACTIVITY DURING ENTORHINAL SHARP WAVES. In the preceding analysis, it could be argued that we underestimated the ability of the perirhinal cortex to transfer neocortical and

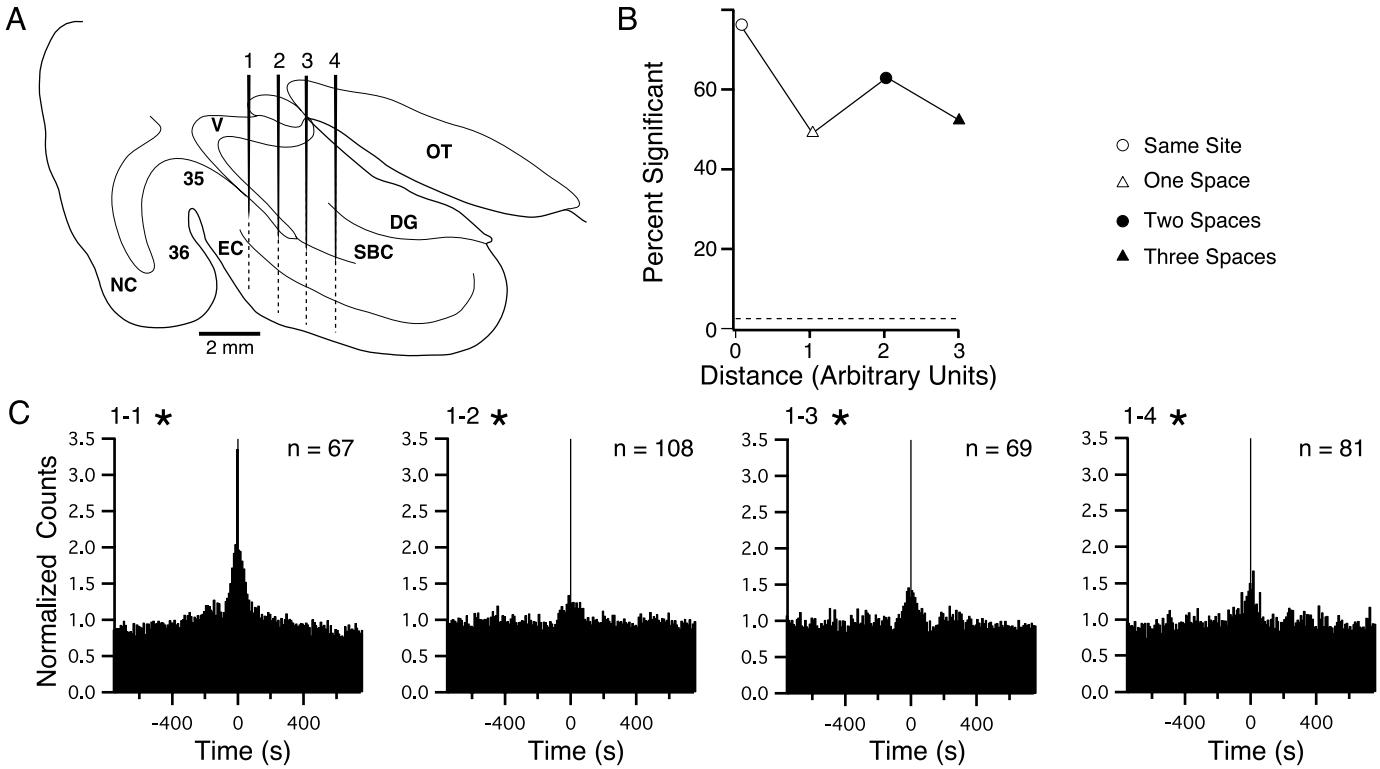

FIG. 5. Synchronized neuronal activity in the entorhinal cortex during SWS. *A*: microelectrode configuration. *B*: graph plotting the proportion of crosscorrelograms with significant positive deviations (*y*-axis) from average bin values. A significance threshold of ±2.8 SDs was used. *C*: population crosscorrelograms. For all pairs of simultaneously recorded entorhinal neurons, crosscorrelograms were computed, normalized to 1, and averaged as a function of the position of the reference and target cells (numbers in the *upper left hand corner* of histograms). Asterisks indicate histograms with a significantly elevated bin within ±50 ms of the origin (paired *t*-test, $P < 0.05$). Numbers on the *top right* of the histograms indicate the number of cell pairs included in each analysis.

entorhinal inputs because we considered all spontaneous activity. Indeed, it is possible that the perirhinal cortex only transfers inputs arising from large groups of neurons activated within a narrow time window. To examine this possibility, we computed PEHs of neuronal discharges around large negative EEG events that occurred spontaneously in the entorhinal cortex during SWS: sharp waves (Chrobak and Buzsáki 1994, 1996). These entorhinal EEG events had to meet the following criteria to be included in the analysis. First, they had to be ≥1.5 mV in amplitude, last ≤250 ms at half-amplitude, and be associated with visually obvious increases in firing rate (Fig. 6). During selection of entorhinal sharp waves, the observer was blind to the neuronal activity taking place at other recording sites.

Figure 7*A* shows the result of this analysis. The entorhinal site used for sharp wave detection was the most medially located recording site (Fig. 7*A6*; *electrode 6* in the *scheme* of Fig. 4*A*). PEHs of neuronal discharges were computed for all available cells in all experiments. Before pooling, the weight of individual PEHs was adjusted as a function of the number of detected entorhinal sharp waves. Then, the population PEH was normalized so that the average bin count = 1.

In the reference site (Fig. 7*A6*), entorhinal sharp waves were associated to an average >6-fold increase in firing rate (*t*-test, $P < 0.05$). At more lateral recording sites, this increase in firing rate quickly diminished (Fig. 7, *A4–A5*), vanishing completely in area 36 (Fig. 7*A3*). No trace of entorhinal sharp wave–related activity could be detected in neocortical recording sites (Fig. 7, *A1–A2*).

To determine whether the failure of entorhinal sharp wave–related activity to propagate beyond the rhinal sulcus resulted only from distance, by opposition to an active gating mechanism, we performed an analogous analysis using synchronized

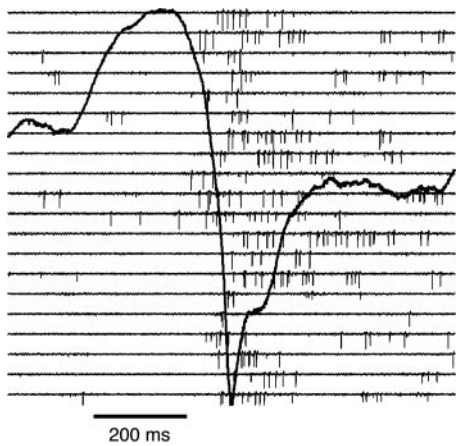

FIG. 6. Firing rate of entorhinal neurons increased during entorhinal sharp waves. Twenty negative focal potentials ≥1.5 mV in amplitude and lasting ≤250 ms were detected visually in the entorhinal cortex and averaged using their peak as a temporal reference (thick line). Data picked up by the electrode were digitally filtered (0.3–20 kHz) to isolate unit activity. Twenty traces illustrate the variations in firing rate that occurred during entorhinal sharp waves.

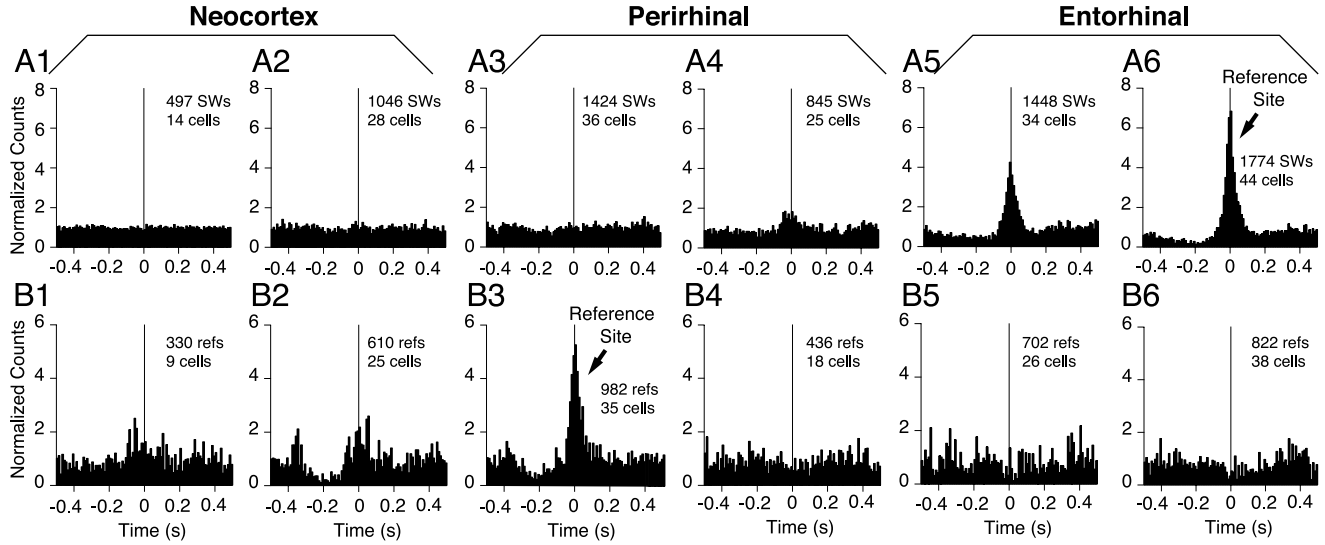

FIG. 7. Perievent histograms of spontaneous firing for cells recorded in the neocortex (*1–2*), perirhinal cortex (*3–4*), and entorhinal cortex (*5–6*). *A*: temporal reference was the negative peak of the entorhinal sharp waves detected in the most medial microelectrode (*A6*) as depicted in Fig. 4. *B*: temporal reference was the negative peak of similar EEG potentials detected in the most lateral perirhinal microelectrode (*B3*; see text) as depicted in Fig. 4. Abbreviations: refs, EEG reference peaks; SWs, sharp waves.

EEG events recorded in area 36 as a temporal reference. As was the case for the above analysis, we detected large-amplitude ($\geq$1.5 mV) negative EEG events lasting $\leq$250 ms at half-amplitude, and associated with visually obvious increases in firing rate. The procedure used to compute and normalize population PEHs was the same as in the previous case (Fig. 7*A*).

Figure 7*B* shows the result of this analysis. Population PEHs look more noisy than in Fig. 7*A* because a lower number of EEG events met our selection criteria. Nevertheless, in the perirhinal site used for detection of the sharp EEG events (Fig. 7*B3*), a large increase in average firing rate was apparent around the origin (peak increase of 3.91 over baseline; *t*-test, $P < 0.05$). Some evidence of this could be seen in adjacent neocortical recording sites (Fig. 7, *B1–B2*), albeit more subtle. In contrast, in more medial recording sites (in area 35 and the entorhinal cortex), no increase in firing rate could be detected around the origin (Fig. 7, *B4–B6*).

DISCUSSION

Using electrical stimulation and crosscorrelation of spontaneous activity, the present study provides evidence that perirhinal transmission of neocortical and entorhinal inputs occurs with a low probability. Even synchronized neuronal discharges such as those occurring spontaneously in relation to entorhinal sharp waves failed to propagate across the perirhinal cortex. In the following account, we will consider the significance of these findings in light of recent studies on the physiology of the perirhinal cortex.

Low-probability perirhinal transmission of neocortical and entorhinal inputs

There is physiological evidence, albeit controversial, that the perirhinal cortex projects, by way of the entorhinal cortex, to the dentate gyrus (for an overview of the debate see Canning and Leung 1997, 1999; Liu and Bilkey 1998; Naber et al. 1999; Witter et al. 1999). Although we did not test this question directly, our results do not support this possibility, given that neocortical stimulation rarely activated entorhinal neurons.

Nevertheless, our conclusions are in agreement with a series of previous in vitro findings. For instance, in the whole guinea pig brain kept in vitro, electrical stimulation of the lateral olfactory tract was reported to evoke massive neuronal excitation in the entorhinal cortex but no local field response in area 36 (Biella et al. 2003). Similarly, stimulation of the temporal neocortex or area 36 evoked no local field responses in the entorhinal cortex, whereas stimulation of area 35 elicited postsynaptic potentials (PSPs) in a low proportion of intracellularly recorded entorhinal cells (Biella et al. 2002).

Moreover, imaging studies of intrinsic (Frederico et al. 1994) and voltage-sensitive signals (Biella et al. 2003; de Curtis et al. 1999) yielded results identical to those obtained with field potential recordings. Indeed, entorhinal optical signals generated by stimulation of the lateral olfactory tract or hippocampus never propagated lateral to the rhinal fissure. However, intracellular recordings revealed that a few entorhinal cells display excitatory postsynaptic potentials (EPSPs) in response to stimuli applied in area 36 or area 35 (Biella et al. 2003).

Thus there appears to be a discrepancy between anatomical findings, showing strong reciprocal connections between the perirhinal and entorhinal cortices, and physiological data about this pathway. In light of these data, it appears unlikely that correlations seen between electroencephalographic events of the somatosensory cortex and hippocampus (Siapas and Wilson 1998; Sirota et al. 2003) depend on a stepwise progression of impulses through the rhinal cortices. Other routes, such as the midline thalamus (Dolleman-Van der Weel et al. 1996, 1997; Wouterlood et al. 1990) and medial prefrontal cortex (Condé et al. 1995; Hurley et al. 1991), are probably involved. The amygdala is an unlikely candidate because it does not display sleep spindles (reviewed in Paré et al. 2002).

Below, we consider some of the factors that might explain transmission failure across the rhinal fissure.

Factors limiting impulse traffic across the perirhinal cortex

LOCAL INHIBITION. Although synaptic inhibition is ubiquitous in the cerebral cortex, our findings suggest that it plays a particularly important role in the perirhinal cortex. As was reported in other cortical regions (Dutar and Nicoll 1988; McCormick 1989; Scanziani et al. 1991), principal perirhinal neurons display $GABA_A$ and $GABA_B$ responses (Biella et al. 2001; Garden et al. 2002; Martina et al. 2001).

We submit that the solution to the low-probability perirhinal transfer of impulses resides in the way GABAergic cells of the perirhinal cortex are recruited by neocortical and entorhinal inputs. As mentioned in the INTRODUCTION, the progression of impulses through discrete steps (neocortex to area 36 to area 35 to entorhinal cortex and conversely) is not perfect because some deep neocortical neurons project beyond area 36 into area 35 and the lateral EC (Burwell and Amaral 1998a,b; Insausti et al. 1987; McIntyre et al. 1996; Saleem and Tanaka 1996; Suzuki and Amaral 1994; VanHoesen and Pandya 1975). Moreover, some entorhinal axons extend to area 35 and the temporal neocortex (Burwell and Amaral 1998b; Deacon et al. 1983; Insausti et al. 1997; Suzuki and Amaral 1994; Swanson and Köhler 1986).

Thus progression of impulses through the rhinal cortices occurs in 2 ways: most of the connections involve a relatively slow stepwise progression through a sequence of cortical areas, but a minor proportion of axons "jump ahead." We hypothesize that the latter either originate in *1*) GABAergic cells that contact principal neurons or *2*) in glutamatergic cells that mainly contact GABAergic interneurons. Because the direct mode of communication is faster than the more prevalent stepwise mode, GABAergic inhibitory PSPs generated by the fast route will precede EPSPs generated by the slow path. As a result, the probability of transfer through the slow path will be severely reduced. Although these predictions await testing with tract tracing coupled to GABA immunocytochemistry at the electron microscopic level, preliminary intracellular recordings of entorhinal neurons in vivo support this hypothesis (unpublished observations).

It is also possible that entorhinal neurons contribute to gate impulse traffic between the neocortex and hippocampus. Consistent with this, physiological studies have disclosed the existence of powerful inhibitory pressures in the entorhinal cortex (Finch et al. 1986, 1988; Funahashi and Stewart 1998; Heinemann et al. 2000; Jones 1990; Jones and Buhl 1992).

INTRINSIC MEMBRANE PROPERTIES OF PERIRHINAL NEURONS. Another factor that may exert an impact on the transfer properties of the perirhinal cortex is the presence of "late-firing" neurons (Faulkner and Brown 1999). In these cells, there is a conspicuous delay between the onset of depolarizing current pulses and spike discharges. This behavior results from a slowly inactivating K^+ conductance that activates around -65 mV (Bargas et al. 1989; Hammond and Crépel 1992; Martina et al. 1999; Nisenbaum et al. 1994; Storm 1988). This current attenuates and delays depolarizing voltage transients caused by excitatory synaptic inputs. Because late-firing cells are particularly abundant in layer VI (86% of the cells according to McGann et al. 2001), and deep neurons contribute most perirhinal projections to the neocortex, this property may be detrimental to the transfer of entorhinal inputs to the neocortex. The presence of late-firing cells in perirhinal layer III (Beggs et al. 2000) suggests that this property might interfere with propagation of neocortical inputs toward the entorhinal cortex.

Gating of impulse traffic through the rhinal cortices

Our results suggest that, in the behavioral states investigated here, there is little communication between the temporal neocortex and hippocampus through the rhinal cortices. Our findings suggest that the rhinal cortices are more than a relay between neocortex and hippocampus, but rather a gating or filtering network whose properties remain to be identified. Moreover, the fact that sharp wave–related entorhinal activity failed to propagate through the perirhinal cortex suggests that the hippocampal replay of waking memories in SWS (Buzsáki 1989; Pennartz et al. 2002) is a local phenomenon, or at least, that it does not affect the neocortex through the rhinal cortices. Alternatively, it is possible that transfer of replayed sequences involves such a small and spatially distributed group of rhinal neurons, that it could not be detected with the methods used here. At the very least, our results imply that communication between hippocampus and neocortex does not involve large populations of rhinal cells.

However, the critical question is whether the inhibitory control of perirhino-entorhinal communication is ever lifted and, if so, how. Recently, it was reported that amygdala inputs could promote the spread of perirhinal activity to the entorhinal cortex and hippocampus in conditions of partial $GABA_A$ block (Kajiwara et al. 2003). Thus it is conceivable that afferents to the rhinal cortices, by reducing inhibition, might facilitate impulse traffic in this circuit. Although the identity of these afferents remains unknown, likely possibilities include the basolateral amygdala and the medial prefrontal cortex. Indeed, the basolateral amygdala sends a glutamatergic projection to the perirhinal and entorhinal cortices (Krettek and Price 1977a,b; Room and Groenewegen 1986; Smith and Paré, 1994; reviewed in Pitkanen et al. 2000). As for the medial prefrontal cortex, it sends robust projections to the rhinal cortices (Room et al. 1985; Sesack et al. 1989; Takagishi and Chiba 1991).

In conclusion, our findings imply that, in some circumstances at least, the perirhinal cortex operates independently of the entorhinal–hippocampal system and is thus in a position to perform distinct computations.

GRANTS

This work was supported by National Institute of Mental Health Grant RO1MH-066856-01 to D. Paré and a Fonds de la Recherche en Santé du Québec fellowship to J. Guillaume Pelletier.

REFERENCES

Bargas J, Galarraga E, and Aceves J. An early outward conductance modulates the firing latency and frequency of neostriatal neurons of the rat brain. *Exp Brain Res* 75: 146–156, 1989.

Beggs JM, Moyer JR Jr, McGann JP, and Brown TH. Prolonged synaptic integration in perirhinal cortical neurons, *J Neurophysiol* 83: 3294–3298, 2000.

Biella G, Uva L, and de Curtis M. Network activity evoked by neocortical stimulation in area 36 of the guinea pig perirhinal cortex. *J Neurophysiol* 86: 164–172, 2001.

Biella G, Uva L, and de Curtis M. Propagation of neuronal activity along the neocortical-perirhinal-entorhinal pathway in the guinea pig. *J Neurosci* 22: 9972–9979, 2002.

Biella JR, Gnatkovsky V, Takashima I, Kajiwara R, Iijima T, and de Curtis M. Olfactory input to the parahippocampal region of the isolated guinea pig brain reveals weak entorhinal to perirhinal interactions. *Eur J Neurosci* 18: 95–101, 2003.

Brown MW and Aggleton JP. Recognition memory: what are the roles of the perirhinal cortex and hippocampus? *Nat Rev Neurosci* 2: 51–61, 2001.

Burwell RD and Amaral DG. Cortical afferents of the perirhinal, postrhinal, and entorhinal cortices of the rat. *J Comp Neurol* 398: 179–205, 1998a.

Burwell RD and Amaral DG. Perirhinal and postrhinal cortices of the rat: interconnectivity and connections with the entorhinal cortex. *J Comp Neurol* 391: 293–321, 1998b.

Burwell RD and Witter MP. Basic anatomy of the parahippocampal region in monkeys and rats. In: *The Parahippocampal Region*, edited by Witter MP and Wouterlood F. New York: Oxford Univ. Press, 2002, p. 35–53.

Buzsáki G. Two-stage model of memory trace formation: a role for "noisy" brain states. *Neuroscience* 31: 551–570, 1989.

Buzsáki G, Leung LW, and Vanderwolf CH. Cellular bases of hippocampal EEG in the behaving rat. *Brain Res Rev* 287: 139–171, 1983.

Canning KJ and Leung LS. Lateral entorhinal, perirhinal, and amygdala-entorhinal transition projections to hippocampal CA1 and dentate gyrus in the rat: a current source density study. *Hippocampus* 7: 643–655, 1997.

Canning KJ and Leung LS. Current source density analysis does not reveal a direct projection from the perirhinal cortex to septal part of hippocampal CA1 or dentate gyrus. *Hippocampus* 9: 599–600, 1999.

Chrobak JJ and Buzsáki G. Selective activation of deep layer (V–VI) retrohippocampal cortical neurons during hippocampal sharp waves in the behaving rat. *J Neurosci* 14: 6160–6170, 1994.

Chrobak JJ and Buzsáki G. High-frequency oscillations in the output networks of the hippocampal-entorhinal axis of the freely behaving rat. *J Neurosci* 16: 3056–3066, 1996.

Collins DR and Paré D. Reciprocal changes in the firing probability of lateral and central medial amygdala neurons. *J Neurosci* 19: 836–844, 1999.

Condé F, Maire-Lepoivre E, Audinat E, and Crepel F. Afferent connections of the medial frontal cortex of the rat. II. Cortical and subcortical afferents. *J Comp Neurol* 352: 567–593, 1995.

Deacon TW, Eichenbaum H, Rosenberg P, and Eckmann KW. Afferent connections of the perirhinal cortex in the rat. *J Comp Neurol* 220: 168–190, 1983.

de Curtis M, Takashima I, and Iijima T. Optical recording of cortical activity after in vitro perfusion of cerebral arteries with a voltage-sensitive dye. *Brain Res* 837: 314–319, 1999.

Dolleman-Van der Weel MJ, Lopes da Silva FH, and Witter MP. Nucleus reuniens thalami modulates activity in hippocampal field CA1 through excitatory and inhibitory mechanisms. *J Neurosci* 17: 5640–5650, 1997.

Dolleman-Van der Weel MJ and Witter MP. Projections from the nucleus reuniens thalami to the entorhinal cortex, hippocampal field CA1, and the subiculum in the rat arise from different populations of neurons. *J Comp Neurol* 364: 637–650, 1996.

Dutar P and Nicoll RA. A physiological role for GABA B receptors in the central nervous system. *Nature* 332: 156–158, 1988.

Faulkner B and Brown TH. Morphology and physiology of neurons in the rat perirhinal-lateral amygdala area. *J Comp Neurol* 411: 613–642, 1999.

Federico P, Borg SG, Salkauskus AG, and MacVicar BA. Mapping patterns of neuronal activity and seizure propagation by imaging intrinsic optical signals in the isolated whole brain of the guinea-pig. *Neuroscience* 58: 461–480, 1994.

Finch DM, Tan AM, and Isokawa-Akesson M. Feedforward inhibition of the rat entorhinal cortex and subicular complex. *J Neurosci* 8: 2213–2226, 1988.

Finch DM, Wong EE, Derian EL, and Babb TL. Neurophysiology of limbic system pathways in the rat: projections from the subicular complex and hippocampus to the entorhinal cortex. *Brain Res* 397: 205–213, 1986.

Funahashi M and Stewart M. GABA receptor-mediated post-synaptic potentials in the retrohippocampal cortices: regional, laminar and cellular comparisons. *Brain Res* 787: 19–33, 1998.

Garden DLF, Kemp N, and Bashir ZI. Differences in GABAergic transmission between two inputs into the perirhinal cortex. *Eur J Neurosci* 16: 437–444, 2002.

Hammond C and Crépel F. Evidence for a slowly inactivating K^+ current in prefrontal cortical cells. *Eur J Neurosci* 4: 1087–1092, 1992.

Heinemann U, Schmitz D, Eder C, and Gloveli T. Properties of entorhinal cortex projection cells to the hippocampal formation. *Ann NY Acad Sci* 911: 112–126, 2000.

Hurley KM, Herbert H, Moga MM, and Saper CB. Efferent projections of the infralimbic cortex of the rat. *J Comp Neurol* 308: 249–276, 1991.

Insausti R, Amaral DG, and Cowan WM. The entorhinal cortex of the monkey. II. Cortical afferents. *J Comp Neurol* 264: 356–395, 1987.

Insausti R, Herrero MT, and Witter MP. Entorhinal cortex of the rat: cytoarchitectonic subdivisions and the origin and distribution of cortical efferents. *Hippocampus* 7: 146–183, 1997.

Jones RSG. Synaptic transmission between layers V–VI and layer II of the rat medial entorhinal cortex in vitro. *J Physiol* 429: 47P, 1990.

Jones RSG and Buhl EH. Synaptic and intrinsic responses of morphologically identified basket neurons in layer II of the rat entorhinal cortex in vitro. *J Physiol* 446: 257P, 1992.

Kajiwara R, Takashima I, Mimura Y, and Iijima T. Amygdala input promotes spread of excitatory neural activity from perirhinal cortex to the entorhinal–hippocampal circuit. *J Neurophysiol* 89: 2176–2184, 2003.

Krettek JE and Price JL. Projections from the amygdaloid complex to the cerebral cortex and thalamus in the rat and cat. *J Comp Neurol* 172: 687–722, 1977a.

Krettek JE and Price JL. Projections from the amygdaloid complex and adjacent olfactory structures to the entorhinal cortex and to the subiculum in the rat and cat. *J Comp Neurol* 172: 723–752, 1977b.

Liu P and Bilkey DK. Is there a direct projection from perirhinal cortex to the hippocampus? *Hippocampus* 8: 424–425, 1998.

Martina M, Royer S, and Paré D. Physiological properties of central medial and central lateral amygdala neurons. *J Neurophysiol* 82: 1843–1854, 1999.

Martina M, Royer S, and Paré D. Cell-type-specific GABA responses and chloride homeostasis in the cortex and amygdala. *J Neurophysiol* 86: 2887–2895, 2001.

McCormick DA. GABA as an inhibitory transmitter in human cerebral cortex. *J Neurophysiol* 62: 1018–1027, 1989.

McGann JP, Moyer J Jr, and Brown TH. Predominance of late-spiking neurons in layer VI of rat perirhinal cortex. *J Neurosci* 21: 4969–4976, 2001.

McIntyre DC, Kelly ME, and Staines WA. Efferent projections of the anterior perirhinal cortex in the rat. *J Comp Neurol* 369: 302–318, 1996.

Murray WA and Richmond BJ. Role of perirhinal cortex in object perception, memory, and associations. *Curr Opin Neurobiol* 11: 188–193, 2001.

Naber PA, Witter MP, and Lopes da Silva FH. Perirhinal cortex input to the hippocampus in the rat: evidence for parallel pathways, both direct and indirect. A combined physiological and anatomical study. *Eur J Neurosci* 11: 4119–4133, 1999.

Nadasdy Z, Hirase H, Czurko A, Csicsvari J, and Buzsáki G. Replay and time compression of recurring spike sequences in the hippocampus. *J Neurosci* 19: 9497–9507, 1999.

Nisenbaum ES, Xu ZC, and Wilson CJ. Contribution of a slowly inactivating potassium current to the transition to firing of neostriatal spiny projection neurons. *J Neurophysiol* 71: 1174–1189, 1994.

Paré D, Collins DR, and Pelletier JG. . Amygdala oscillations and the consolidation of emotional memories. *Trends Cogn Sci* 6: 306–314, 2002.

Pennartz CM, Uylings HB, Barnes CA, and McNaughton BL. Memory reactivation and consolidation during sleep: from cellular mechanisms to human performance. *Prog Brain Res* 138: 143–166, 2002.

Pitkanen A, Pikkarainen M, Nurminen N, and Ylinen A. Reciprocal connections between the amygdala and the hippocampal formation, perirhinal cortex, and postrhinal cortex in rat. A review. *Ann NY Acad Sci* 911: 369–391, 2000.

Room P and Groenewegen HJ. Connections of the parahippocampal cortex. I. Cortical afferents. *J Comp Neurol* 251: 415–450, 1986.

Room P, Russchen FT, Groenewegen HJ, and Lohman AH. Efferent connections of the prelimbic (area 32) and the infralimbic (area 25) cortices: an anterograde tracing study in the cat. *J Comp Neurol* 242: 40–55, 1985.

Saleem KS and Tanaka K. Divergent projections from the anterior inferotemporal area TE to the perirhinal and entorhinal cortices in the macaque monkey. *J Neurosci* 16: 4757–4775, 1996.

Scanziani M, Gähwiler BH, and Thompson SM. Paroxysmal inhibitory potentials mediated by GABAB receptors in partially disinhibited rat hippocampal slice cultures. *J Physiol* 444: 375–396, 1991.

Sesack SR, Deutch AY, Roth RH, and Bunney BS. Topographical organization of the efferent projections of the medial prefrontal cortex in the rat: an anterograde tract-tracing study with Phaseolus vulgaris leucoagglutinin. *J Comp Neurol* 290: 213–242, 1989.

Shadlen MN and Newsome WT. The variable discharge of cortical neurons: implications for connectivity, computation, and information coding. *J Neurosci* 18: 3870–3896, 1998.

Siapas AG and Wilson MA. Coordinated interactions between hippocampal ripples and cortical spindles during slow-wave sleep. *Neuron* 21: 1123–1128, 1998.

Sirota A, Csicsvari J, Buhl D, and Buzsáki G. Communication between neocortex and hippocampus during sleep in rodents. *Proc Natl Acad Sci USA* 100: 2065–2069, 2003.

Skaggs WE and McNaughton BL. Replay of neuronal firing sequences in rat hippocampus during sleep following spatial experience. *Science* 271: 1870–1873, 1996.

Smith Y and Paré D. Intra-amygdaloid projections of the lateral nucleus in the cat: PHA-L anterograde labeling combined with post-embedding GABA and glutamate immunocytochemistry. *J Comp Neurol* 342: 232–248, 1994.

Steriade M. Synchronized activities of coupled oscillators in the cerebral cortex and thalamus at different levels of vigilance. *Cereb Cortex* 7: 583–604, 1997.

Steriade M and Hobson JA. Neuronal activity during the sleep-waking cycle. *Prog Neurobiol* 6: 155–376, 1976.

Stevens CF and Zador AM. Input synchrony and irregular firing of cortical neurons. *Nat Neurosci* 1: 210–217, 1998.

Storm JF. Temporal integration by a slowly inactivating K^+ current in hippocampal neurons. *Nature* 336: 379–381, 1988.

Sutherland GR and McNaughton B. Memory trace reactivation in hippocampal and neocortical neuronal ensembles. *Curr Opin Neurobiol* 10: 180–186, 2000.

Suzuki WA. The anatomy, physiology and functions of the perirhinal cortex. *Curr Opin Neurobiol* 6: 179–186, 1996.

Suzuki WA and Amaral DG. Topographic organization of the reciprocal connections between the monkey entorhinal cortex and the perirhinal and parahippocampal cortices. *J Neurosci* 14: 1854–1877, 1994.

Swanson LW and Kohler C. Anatomical evidence for direct projections from the entorhinal area to the entire cortical mantle in the rat. *J Neurosci* 6: 3010–3023, 1986.

Takagishi M and Chiba T. Efferent projections of the infralimbic (area 25) region of the medial prefrontal cortex in the rat: an anterograde tracer PHA-L study. *Brain Res* 566: 26–36, 1991.

Van Hoesen GW and Pandya DN. Some connections of the entorhinal (area 28) and perirhinal (area 35) cortices of the rhesus monkey. I. Temporal lobe afferents. *Brain Res* 95: 1–24, 1975.

Wilson MA and McNaughton BL. Reactivation of hippocampal ensemble memories during sleep. *Science* 265: 676–679, 1994.

Witter MP and Groenewegen HJ. Connections of the parahippocampal cortex in the cat. III. Cortical and thalamic efferents. *J Comp Neurol* 252: 1–31, 1986.

Witter MP, Naber PA, and Lopes da Silva F. Perirhinal cortex does not project to the dentate gyrus. *Hippocampus* 9: 605–606, 1999.

Witter MP, Room P, Groenewegen HJ, and Lohman AHM. Connections of the parahippocampal cortex in the cat. V. Intrinsic connections: comments on input/output connections with the hippocampus. *J Comp Neurol* 252: 78–94, 1986.

Witter MP, Wouterlood FG, Naber PA, and Van Haeften T. Anatomical organization of the parahippocampal–hippocampal network. *Ann NY Acad Sci* 911: 1–24, 2000.

Wouterlood FG, Saldana E, and Witter MP. Projection from the nucleus reuniens thalami to the hippocampal region: light and electron microscopic tracing study in the rat with the anterograde tracer Phaseolus vulgaris-leucoagglutinin. *J Comp Neurol* 296: 179–203, 1990.